Experimental determination of solid–liquid surface energy for Cd solid solution in Cd–Zn liquid solutions

2006 J. Phys.: Condens. Matter 18 10143

(http://iopscience.iop.org/0953-8984/18/45/003)

INSTITUTE OF PHYSICS PUBLISHING JOURNAL OF PHYSICS: CONDENSED MATTER

J. Phys.: Condens. Matter **18** (2006) 10143–10155 doi:10.1088/0953-8984/18/45/003

Experimental determination of solid–liquid surface energy for Cd solid solution in Cd–Zn liquid solutions

B Saatçi[1] **and H Pamuk**

Department of Physics, Faculty of Arts and Sciences, Erciyes University, 38039, Kayseri, Turkey

E-mail: bayender@erciyes.edu.tr

Received 2 March 2006, in final form 22 September 2006
Published 26 October 2006
Online at stacks.iop.org/JPhysCM/18/10143

Abstract

The equilibrated grain boundary groove shapes for the Cd solid solution in equilibrium with the Cd–Zn liquid have been observed by rapid quenching. From the observed grain boundary groove shapes, the Gibbs–Thomson coefficient and the solid–liquid surface energy for the Cd solid solution in equilibrium with the Cd–Zn eutectic liquid have been determined to be $(8.16 \pm 0.65) \times 10^{-8}$ K m and (121 ± 16) mJ m^{-2} with the numerical method and from the Gibbs–Thomson equation, respectively. The grain boundary energy for the same material has been calculated as (241 ± 30) mJ m^{-2} from the observed grain boundary groove shapes. The thermal conductivities of the solid and liquid phases for Cd–26.5% Zn and Cd–5% Zn alloys have also been measured.

1. Introduction

The solid–liquid surface energy, σ_{SL}, is defined as the reversible work required to create a unit area of the interface at constant temperature, volume and chemical potentials [1] and it plays a critical role in phase transformations. Many attempts have been made to determine the values of σ_{SL} in various materials by using different methods over the last 50 years. These examples emphasize the importance of σ_{SL} in understanding solid–liquid transformations and in having quantitative values of σ_{SL} involved. Unfortunately, it is not easy to measure σ_{SL} even for a pure material, and very little progress has been made in its measurement for multi-component system.

A technique was developed to measure σ_{SL} in metallic alloy systems by Gündüz and Hunt [2, 3]. The technique was based on equilibrating a grain boundary with a solid–liquid interface in an applied temperature gradient, G. When the planar grain boundary intersects with a stabilized planar solid–liquid interface, a shape of the grain boundary groove is formed (figure 1(a)). It is possible to obtain the Gibbs–Thomson constant, Γ, from the groove shape and this allows calculation of σ_{SL} for the system, provided that the related physical constants

[1] Author to whom any correspondence should be addressed.

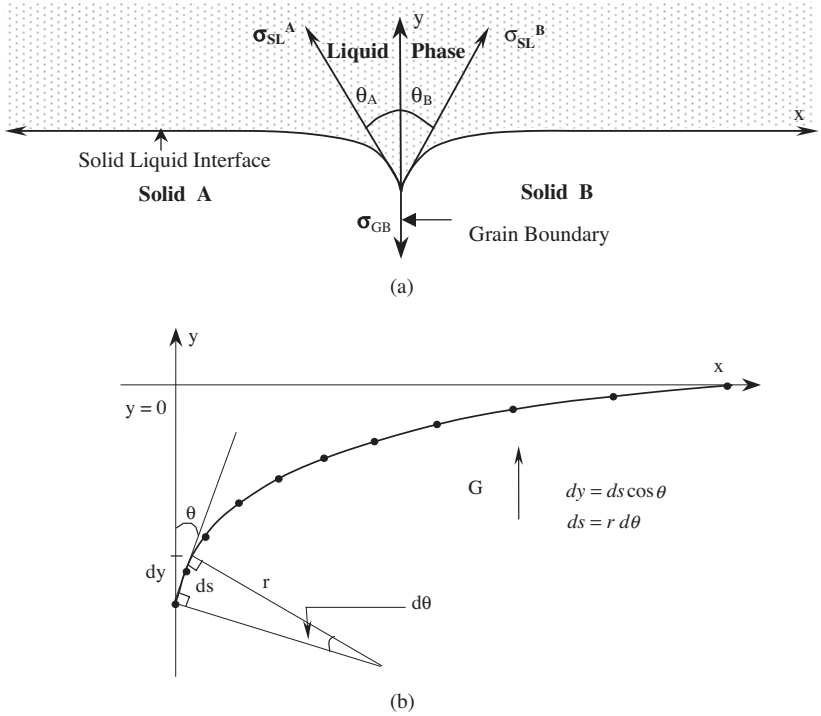

Figure 1. (a) Schematic illustration of an equilibrated grain boundary groove formed at a solid–liquid interface in a temperature gradient, showing the x, y coordinates and θ. (b) The definitions of θ, $\mathrm{d}\theta$, $\mathrm{d}s$, $\mathrm{d}y$, G, points on the groove, x and y.

are known. The Gibbs–Thomson coefficient, Γ, is expressed in the form of a change in undercooling ΔT_r with radius r for a groove as

$$\Delta T_r = \frac{\Gamma}{r(x, y)}. \tag{1}$$

Equation (1) can be integrated in the y direction (perpendicular to the macroscopic interface) from the flat interface to a point on the cusp [2] (figure 1(b)):

$$\int_0^y \Delta T_r \, \mathrm{d}y = \Gamma \int_0^y \frac{1}{r} \, \mathrm{d}y. \tag{2}$$

The left-hand side of equation (2) may be evaluated if ΔT_r is known as a function of y. When the thermal conductivities of the solid (K_S) and liquid (K_L) phases are equal, ΔT_r just depends on G and y, that is $\Delta T_r = Gy$. However, in practice the conductivities of the two phases will not be equal, so that the left-hand side of equation (2) can be integrated numerically using the numerically calculated ΔT_r values [2, 3]. The right-hand side of equation (2) may be evaluated for any shape by defining $\mathrm{d}s = r \, \mathrm{d}\theta$ (where s is the distance along the interface and θ is the angle of the interface to y, which is obtained by fitting a Taylor expansion to the adjacent points on the cusp) giving

$$\int_0^y \frac{1}{r} \, \mathrm{d}y = (1 - \sin\theta). \tag{3}$$

This allows the Gibbs–Thomson coefficient to be determined for a measured grain boundary groove shape. To get accurate values of the Gibbs–Thomson coefficient, the shape of the

interface, the temperature gradient in the solid, G_S, and the conductivities of the solid, (K_S), and liquid, (K_L), phases must be known.

The solid–liquid surface energy is obtained from the thermodynamic definition of the Gibbs–Thomson coefficient, which is expressed as

$$\Gamma = \frac{\sigma_{SL}}{\Delta S_f} \tag{4}$$

where ΔS_f is the effective entropy of melting per unit volume, which must be known.

Gündüz and Hunt [2, 3] performed measurements of the solid–liquid surface energies in Al–Cu, Al–Si, Pb–Sn and Al–Mg eutectic-based systems. Maraşlı and Hunt [4, 5] extended the technique to measure solid–solid surface energies. In addition, they also made measurements in a peritectic system for the first time. They made measurements of solid–solid and solid–liquid surface energies in the Al–$CuAl_2$ and Al–$NiAl_3$ eutectic systems and the Al–Ti peritectic system.

More recently, Bayender *et al* [6, 7], Maraşlı *et al* [8], Keşlioğlu and Maraşlı [9] and Erol *et al* [10] observed the equilibrated grain boundary groove shapes for transparent and opaque materials. They applied Gündüz and Hunt's numerical method to determine Γ, σ_{SL}, and σ_{GB}, for pivalic acid, camphene, succinonitrile and succinonitrile-carbon tetrabromide, Al–Zn and Bi–Cd binary eutectic systems.

The aim of the present work is to determine Γ, σ_{SL} and σ_{GB} for the Cd solid solution in equilibrium with Cd–Zn eutectic liquid from the observed grain boundary groove shapes.

2. Experimental apparatus and method

2.1. Experimental apparatus

To observe the equilibrated grain boundary groove shapes in opaque materials, Gündüz and Hunt designed a radial heat flow apparatus, and the detail of the apparatus is shown in figure 2. Maraşlı and Hunt improved the experimental apparatus for higher temperature [4]. In both experimental apparatuses, the cooling jacket was very close to the outside of the specimen to obtain effective cooling. The high temperature gradient is useful to obtain the grain boundary groove shapes in a shorter annealing time, but it produces small cusp shapes. In the solid–liquid interface energy measurements, a low temperature gradient is desired to obtain the larger cusp shapes.

The crucible consisted of three parts: a cylindrical bore (25 mm inner diameter ID, 30 mm outer diameter OD and 170 mm in length) and the top and bottom lids which were tightly fitted to the cylindrical part. There were usually three stationary thermocouples (inserted in 0.8 mm ID, 1.2 mm OD alumina tube) which were placed 1.0–1.5 mm away from the central alumina tube: two were for measuring the temperature and the other one was for the control unit (for details, see [2, 3, 11]). The moveable thermocouple (inserted in 1 mm ID, 2 mm OD, alumina tube) was placed 10 mm away from the centre. The central heating element was a single Kanthal A_1 wire (typically 1.8 mm diameter and about 210 mm in length) placed inside a thin-walled alumina tube (2 mm ID, 3 mm OD). The end of the wire was threaded and screwed into 7 mm copper rods. The outside of the cylindrical crucible (sample) was kept cool by the water-cooled jacket. The jacket was placed in an alumina tube (85 mm ID, 100 mm OD and 600 mm in length). Kanthal A_1 resistance wire was wound on the alumina tube to obtain an outer heater which gives a hot zone of 300 mm. The inner heater temperature was controlled by a Euroterm type 9706 controller and the outer one was controlled by a Euroterm 815 P controller using K-type (0.5 mm thick insulated chromel–alumel) thermocouples. The potential difference between the ends of the central heating element and the known resistance were checked with

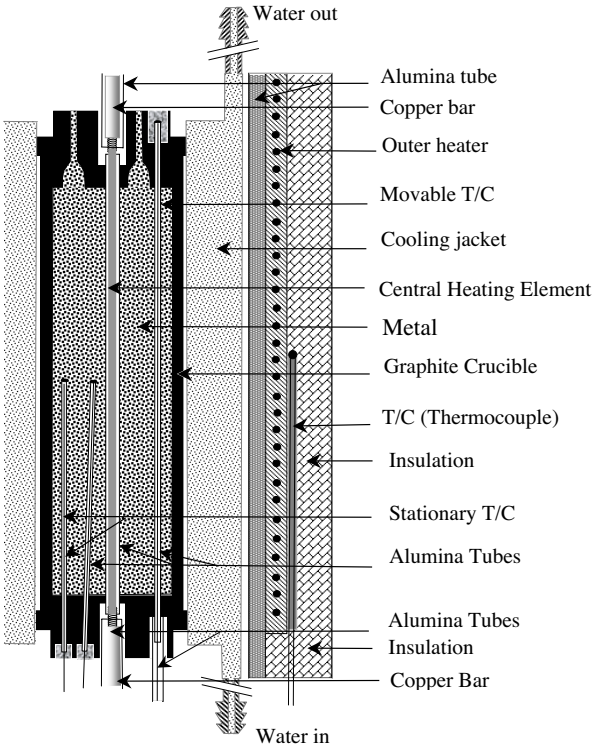

Figure 2. Schematic illustration of the apparatus.

Keithley 2000 and Hewlett Packard 34401 multimeters. Cd–Zn alloys were prepared in a vacuum melting furnace from 4N Cd and Zn. After several stirrings, the molten alloy was poured into the graphite crucible held in a hot filling furnace which was set at approximately 50 K above the eutectic temperature, T_E, of the alloy (539 K). The alloy was then directionally solidified from bottom to top to ensure that the crucible was completely filled. The sample was then taken out of the hot filling furnace, all thermocouples and the inner heating element were placed in the sample, and the sample was inserted in the cooling jacket, then the cooling jacket was placed in the radial heat flow apparatus. The apparatus is capable of holding the sample to within ± 0.05 K for a day and ± 0.1 K for up to a week. The apparatus could be operated either to give relatively a low temperature gradient case (0–1 K cm^{-1}; the inner and the outer heaters were used together without water cooling) or to give a higher temperature gradient case (10–20 K cm^{-1}; only the inner heater was used with water cooling). The temperatures were calibrated *in situ* with the low temperature gradient case. The sample was heated up to 5 K below T_E using the outer heater, and then thermocouples were calibrated by recording T_E during a very slow heating using the inner heater.

The equilibrating time had to be obtained experimentally. Several experiments were carried out to obtain the necessary equilibrating time. The time to reach equilibrium for the Cd solid solution with the Cd–Zn eutectic liquid was found to be between 5 and 14 days, depending on the liquid thickness. After the calibration, the sample was annealed for about 14 days using the high temperature gradient case to ensure that droplets in the semi-solid region migrated to the solid–liquid interface by TGZM (temperature gradient zone melting). During the annealing period, the sample was kept in a low argon pressure. The temperature of the

stationary thermocouples was continuous, and the temperature of the moveable thermocouple and input power were recorded periodically. At the end of the annealing time, the sample was rapidly quenched by turning off the input power, which is sufficient to obtain a well-defined and stationary solid–liquid surface.

2.2. Sample preparation for metallography

When the equilibrated sample was removed from the furnace, the sample was first cut transversely into ∼25 mm lengths and these transverse sections were ground with 180 grid SiC paper before mounting. Grinding and polishing were then carried out using standard techniques. After polishing, the samples were etched with 2% nitric acid in water from 5 to 10 s.

The equilibrated grain boundary groove shapes were then photographed with a CCD digital camera placed on top of an Olympus BH2 light optical microscope using a 50 times objective. A micrometer ($100 \times 0.001 = 10$ mm) was also photographed using the same objective. The digital camera has rectangular pixels. Thus, the magnifications in the x and y directions are different (in this work, COR RJ(J):0.00002459 cm and COR XK(K):0.00002903 cm). The photographs of the equilibrated grain boundary groove shapes and the micrometer in the x and y directions used Adobe Photoshop 7.0 version software, so that accurate measurements of the groove coordinate points on the groove shapes could be made.

2.3. The groove coordinates

In order to obtain accurate Γ values, not only G and K_S values but also coordinates on the grain boundary grooves must be measured accurately. The actual coordinates of the grooves, x, y, z, should be measured on the orthogonal axes x, y, z, where the x-axis is parallel and the y-axis is normal to the flat solid–liquid interface and the z-axis lies at the base of the grain boundary groove. The coordinates x', y' of the grain boundary groove shape can be transformed to x, y by considering the geometry of the grain boundary groove shape in two different planes which are parallel to each other (see details in [4]). Referring to figure 3, d is the distance between the first and second planes along the z'-axis, b is the displacement of the grain boundary position along the x'-axis, a is the displacement of the solid–liquid interface along the y'-axis, α is the angle between the x'-and x-axes, and β is the angle between the y'-and y-axes. Considering the right-angle triangle ABC (see figure 3), the relation between x and x' can be expressed as [5]

$$x = x' \cos\alpha = x' \frac{\sqrt{a^2 + d^2}}{\sqrt{a^2 + b^2 + d^2}} \tag{5}$$

and from the right-angle triangle DEF (see figure 3), the relation between y' and y can be expressed as

$$y = y' \cos\beta = y' \frac{d}{\sqrt{a^2 + d^2}}. \tag{6}$$

As can be seen from equations (5) and (6), if the values of a, b and d are measured, then the groove coordinates, x', y', can be transformed into the x, y coordinates. The required a, b and d measurements were made so that appropriate transformation to the coordinates could be deduced (see detail in [5]).

2.4. Temperature gradient measurements

The temperature gradient at the solid–liquid interface in the solid phase must be measured for each equilibrated groove shape in order to calculate the related Γ. At steady state, the

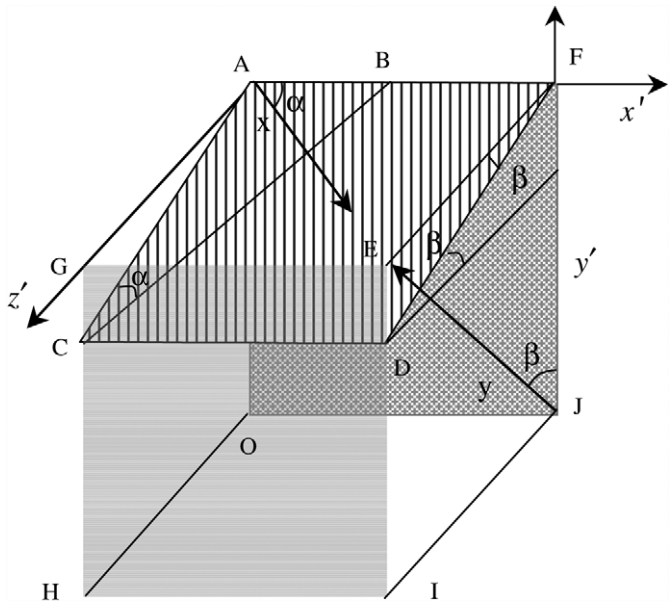

(a)

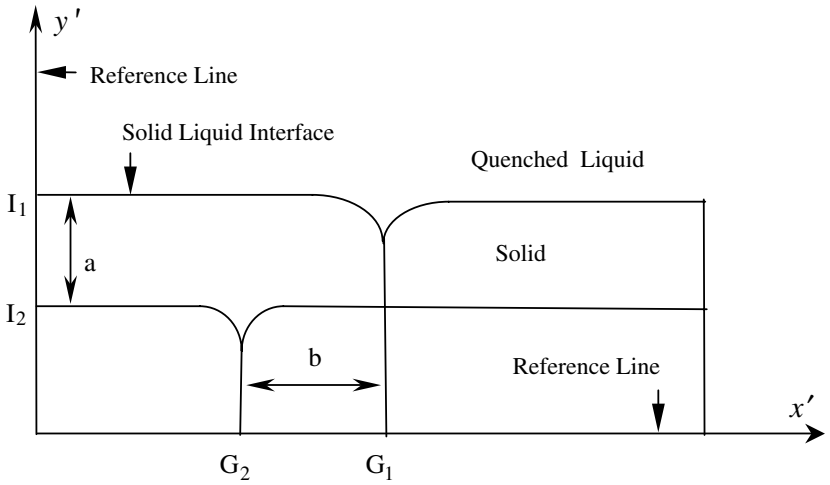

(b)

Figure 3. (a) Schematic illustration for metallic examination of the sample, where B is the location of the grain boundary groove shape on the first plane OJFA, C is the location of the grain boundary groove shape on the second plane HIDC, AB $= b$, CG $=$ ED $= a$ and AG $= d$. (b) Schematic illustration of the displacement of the grain boundary groove shape position along the x'-and y'-axes [4].

temperature gradient at radius r is given by

$$\left(\frac{\mathrm{d}T}{\mathrm{d}r}\right)_s = -\frac{Q}{2\pi r \ell K_S} \tag{7}$$

where Q is input power, ℓ is the length of the heating element, r is the distance of solid–liquid interface to the centre of the sample, and K_S is the thermal conductivity of the solid phase. To obtain a reliable G value from equation (7), it is necessary to measure Q, K_S, and r values as accurately as possible. Q was obtained by measuring the voltage drop across the central single wire heater and the current flowing through the wire.

2.5. Thermal conductivity of the solid phase

In order to calculate the Gibbs–Thomson constant Γ with the numerical method, it is necessary to know the thermal conductivity of the phases. The thermal conductivity of the phases must be measured as accurately as possible, not only to find out the thermal conductivity ratios ($R = K_L/K_S$) but also to calculate the temperature gradient, G, in the solid at the solid–liquid interface. The radial heat flow method has some unique theoretical and practical advantages that, through careful experimental work, can yield reliable results over wide K_S and temperature ranges.

Integration of equation (7) for a cylindrical sample gives

$$K_S = \frac{Q \ln(r_2/r_1)}{2\pi \ell (T_1 - T_2)} \tag{8}$$

where r_1 and r_2 are fixed distances from the centre of the sample, and T_1 and T_2 are temperatures at the fixed positions r_1 and r_2, respectively. If Q, r_1, r_2, ℓ, T_1 and T_2 can be accurately measured for the well-characterized sample, then reliable K_S values can be evaluated.

The samples were heated using the central heating wire in steps of 293–533 K. The samples were kept at steady state from 8 to 12 h. At steady state, the total input power and the temperatures were measured. When all the desired power and temperature measurements were completed, the input power was turned off and the samples were left to cool to room temperature. The process was repeated several times to obtain average values.

The thermal conductivities of solid phases of Cd–26.5 at.% Zn (Cd–Zn eutectic) and the Cd–5 at.% Zn alloys were measured in the radial heat flow apparatus and are shown in figure 4. The values of thermal conductivities which are used in the calculations were obtained by extrapolating the curves at the eutectic temperature (539 K). The value of thermal conductivity of the Cd solid solution (Cd–5 at.% Zn) is obtained as 86 W K^{-1} m^{-1} and the value of thermal conductivity of Cd–Zn eutectic liquid solution (Cd–26.5 at.% Zn) is obtained as 60 W K^{-1} m^{-1}. So, the thermal conductivity ratio R is obtained as 0.70 for the Cd solid solution in Cd–Zn liquid solution.

3. Results and discussion

3.1. The Gibbs–Thomson coefficients

The Gibbs–Thomson coefficient, Γ, for the Cd solid solution Cd–Zn liquid solution was calculated from the measured groove shapes using a numerical method. Details of the numerical program for the calculation of σ_{SL} in the $K_L \neq K_S$ case are given in [2–4]. The calculations were carried out using 10 equilibrated grain boundary groove shapes (figure 5).

The uncorrected Γ and the corrected Γ values were obtained for the Cd solid solution Cd–Zn liquid solution (figures 5, 6 and table 1). The uncorrected Γ values may be used to get an estimate of the magnitude of real Γ values. The values of Γ for the Cd solid solution are given in table 1. The average value of Γ from table 1 is $(8.16 \pm 0.65) \times 10^{-8}$ K m for Cd solution. The error in the Gibbs–Thomson coefficient determinations is estimated to be

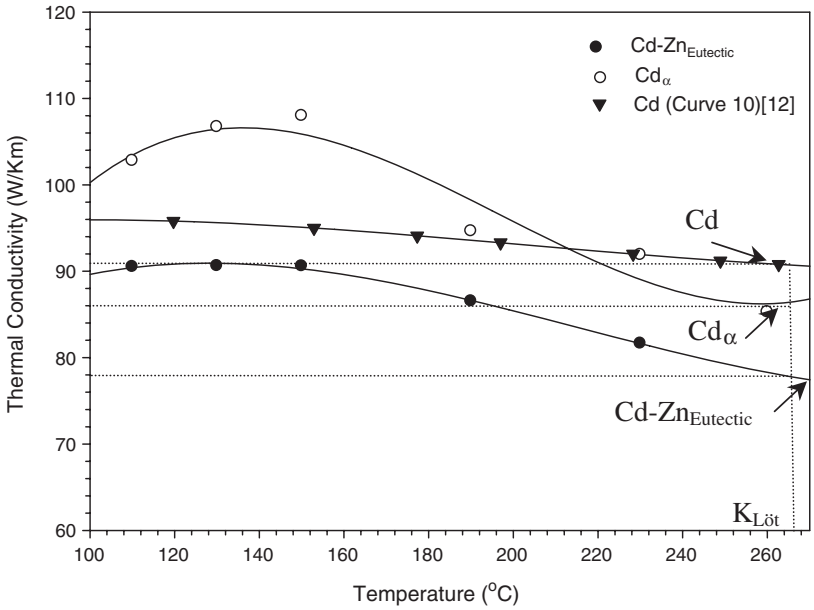

Figure 4. The solid phase thermal conductivities of the Cd–26.5 at.% Zn, Cd–5 at.% Zn alloys and pure Cd [12].

Table 1. Gibbs–Thomson coefficients for the Cd solid solution Cd–Zn liquid solution. (Note: $\Gamma_{Uncorrected} = 10.0 \pm 2.25 \times 10^{-8}$ K m; $\Gamma_{Corrected} = 8.16 \pm 0.65 \times 10^{-8}$ K m.)

				Gibbs–Thomson coefficient $\times 10^{-8}$ (K m)			
Groove no. (see figure 5)	$G_S \times 10^2$ (K m^{-1})	α (deg)	β (deg)	Uncorrected left-hand side	Uncorrected right-hand side	Corrected left-hand side	Corrected right-hand side
A	11.25	39.02	48.11	15.17	15.57	7.86	7.77
B	11.25	34.08	31.52	12.19	12.36	8.63	8.60
C	11.25	28.81	21.24	9.71	8.91	8.14	7.54
D	8.94	21.06	13.97	10.47	9.79	9.24	8.60
E	9.22	6.53	15.87	7.65	8.63	7.14	8.49
F	12.41	10.22	20.62	9.47	9.78	8.81	8.77
G	12.41	0.76	7.86	7.82	8.08	7.72	7.73
H	8.36	40.50	12.57	10.76	9.98	8.59	8.58
İ	9.52	29.63	9.77	8.01	7.72	7.07	6.99
J	11.96	17.69	18.16	9.64	9.08	8.86	8.16

about 8%. This value of Γ is in good agreement with another previous experimental value of $\Gamma(8.28 \pm 0.33) \times 10^{-8}$ K m for the Cd solid solution [13].

3.2. The effective entropy change

To calculate the solid–liquid surface energy, it is also necessary to know the effective entropy change per unit volume. The effective entropy change per unit volume, ΔS_f, for a two-component system is given as [2]

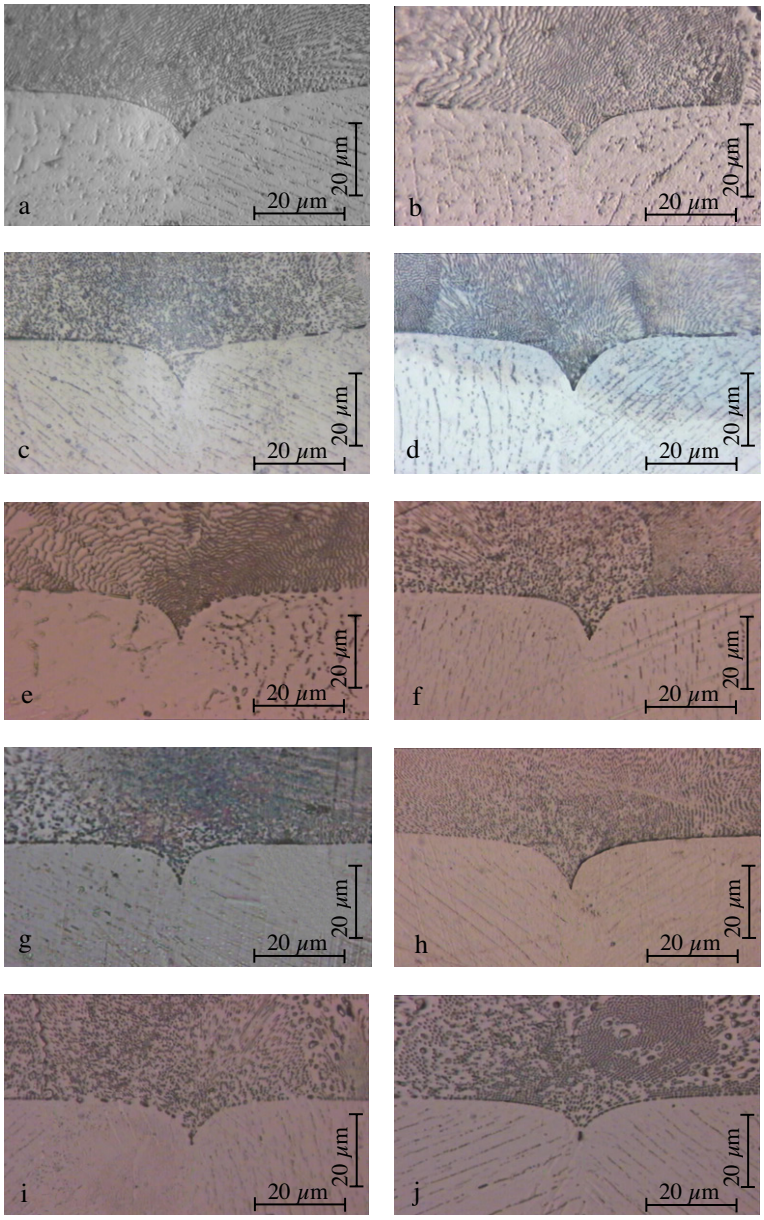

Figure 5. Typical grain boundary groove shape for the Cd solid solution in equilibrium with the Cd–Zn eutectic liquid.

(This figure is in colour only in the electronic version)

$$\Delta S_{\mathrm{f}} = \frac{RT_{\mathrm{E}}(C_{\mathrm{S}} - C_{\mathrm{L}})}{m_{\mathrm{L}} V_{\mathrm{S}}(1 - C_{\mathrm{L}})C_{\mathrm{L}}} \tag{9a}$$

$$\Delta S_{\mathrm{f}} = \frac{RT_{\mathrm{E}}}{m_{\mathrm{L}} V_{\mathrm{S}}} f(C) \tag{9b}$$

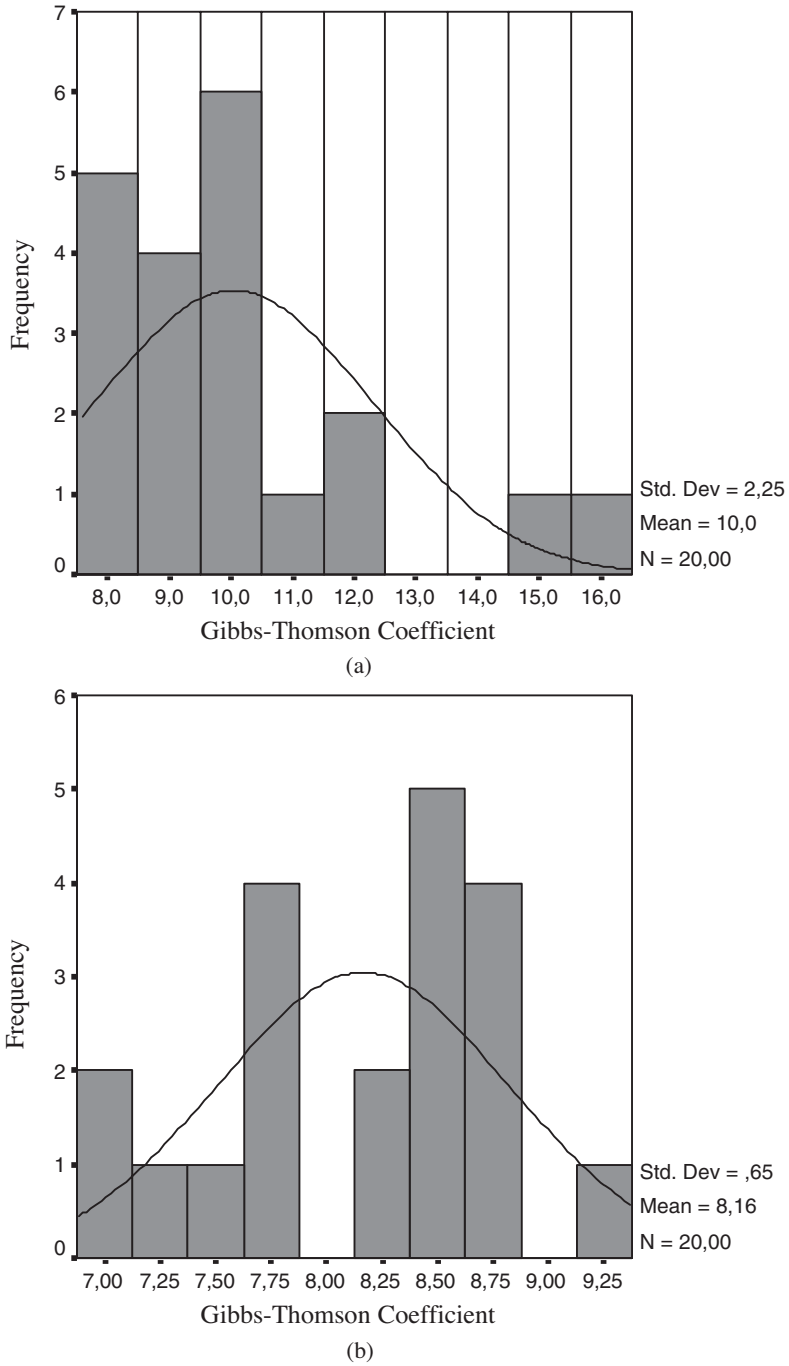

Figure 6. (a) Histogram of the uncorrected Gibbs–Thomson values. (b) Histogram of the corrected Gibbs–Thomson values.

where R is the gas constant, T_E is the eutectic temperature (539 K), C_S and C_L are the compositions of solid and liquid phases in at.%, respectively, V_S is the molar volume, and

Table 2. A comparison of the solid–liquid surface energy measured in the present work with the previous works.

System	Phases		T_E (K)	Solid–liquid surface energy σ_{SL} (mJ m^{-2})
	Solid	Liquid		
Cd	Cd	Cd	594	65.5 [16]
Cd	Cd	Cd	484	66 [17]
			484	81 [17]
			484	85 [17]
Bi–Cd Eutectic	Cd–0.03 at.% Bi	Bi–54.6 at.% Cd	418.7	81.22 ± 7.31 [13]
Cd–Zn Eutectic	Cd–5 at.% Zn	Cd–26.5 at.% Zn	539	121 ± 16 [present work]

m_L is the liquidus slope. The molar volume, V_S is expressed as

$$V_S = V_c N_a \frac{1}{n} \tag{10}$$

where V_c is the volume of the unit cell, N_a is Avogadro's number and n is the number of molecules per unit cell. The obtained value of $f(C)$ is -1.10, m_L is -2.56×10^2 K/at. and V_S is 12.99×10^{-6} m^3 either from density and atomic mass or from lattice parameters and the number of molecules per unit cell. The other parameters (T_E, m_L, C_S and C_L) can be obtained from the relevant phase diagram [14]. As discussed by Tassa and Hunt [15], the biggest uncertainty comes from the measurement of m_L. The uncertainty in ΔS_f due to the uncertainties in the parameters is estimated to be 5%.

3.3. Solid–liquid surface energy, σ_{SL}

If the values of the Gibbs–Thomson coefficient and the entropy of fusion per unit volume are measured, the solid–liquid surface energy can be calculated from equation (4). The value of Γ for the Cd solution Cd–Zn liquid solution was ($8.16 \pm 0.65 \times 10^{-8}$ K m) and the entropy of fusion per unit volume for the same alloy is $1.488 \pm 0.073 \times 10^{-6}$ J/ K per m^3. The value of the solid–liquid surface energy together with the standard deviation is obtained as 121 ± 16 mJ m^{-2}.

The error in Γ was estimated to be 8% and in ΔS_f it was estimated to be about 5%, given a total estimated error for σ_{SL} of about 13%. A comparison with the previous work is shown in table 2. Reasonably good agreement is obtained between the experimental values of σ_{SL} of Cd solid solution with Cd–Zn liquid solution. However, the value σ_{SL} of Cd solid solution is obtained as 65.5 mJ m^{-2} from the radial distribution function and the value σ_{SL} of Cd solid solution is obtained as 81.22 mJ m^{-2} using the same method in Bi–Cd alloy, and the theoretical values of Cd solid solution are obtained as 66, 81, and 85 mJ m^{-2} from the broken bond model, which are smaller than our experimental result.

3.4. The grain boundary energy, σ_{GB}

When σ_{SL} is isotropic, the surface tension is equal to σ_{SL} [1]. By considering the balance of forces at the grain boundary groove, it is possible to determine the solid–solid surface energy and the grain boundary energy, provided that the solid–liquid surface energy is known. When the surface energy is isotropic, the force balance can be expressed as:

$$\sigma_{SS} = \sigma_{SL}^{A} \cos\theta_A + \sigma_{SL}^{B} \cos\theta_B \tag{11}$$

where θ_A and θ_B are the angles that the solid–liquid surfaces make with the y-axis, as shown in figure 1(a). If the grains on either side of the surface are of the same phases, the grain boundary

energy can be expressed as

$$\sigma_{GB} = 2\sigma_{SL}\cos\theta \tag{12}$$

where $\theta = (\theta_A + \theta_B)/2$ is the angle. As can be seen from equation (12), σ_{GB} is not sensitive to the error in θ for small θ values. Even a few degrees error in the angle measurement will not have a significant effect on σ_{GB} when θ is small. In order to calculate σ_{GB} from the groove shapes, the average of θ_A and θ_B was taken as θ. The angles, θ, in the cusp were obtained from the cusp coordinates x, y using a Taylor expansion to the points at the base of the groove. For the cusp measurements to be made, a single-phase solid region must be produced by holding the specimen in a very stable temperature field. Initially, a specimen is placed in a temperature gradient. The liquid droplets on the semi-solid region will move towards the hotter part of the specimen until eventually a single-phase solid is left. The movement is a result of temperature gradient zone melting (TGZM). The rate of motion depends on the temperature gradient. When the alloy has been equilibrated, there is a liquid layer which is almost of eutectic composition, a single solid phase layer which has a composition almost at the limit of solid solubility. In the present work, the problem is to hold a solid–liquid surface in a very stable temperature gradient for a long enough time to produce a macroscopically planar solid–liquid surface except for the grain boundary cusps. In this work, orientations of two grains are not important to us. According to figures 1(a) and (b), grain A is on the left-hand side and grain B is on the right-hand side in the solid phase. In table 1, grain boundary grooves are obtained from different equilibrated samples. The reason why the angles are different is that groove shapes made an angle with grain boundaries. The grain boundary energies were calculated from equation (11) using the related σ_{SL} and θ for ten groove shapes, for the Cd solid solution Cd–Zn liquid solution (figure 5). The grain boundary energy with its standard deviation was found to be $\sigma_{GB} = 241 \pm 30$ mJ m^{-2}. The error is estimated to be about 13% for σ_{GB}.

4. Conclusions

(1) The variation of the thermal conductivity with temperature up to T_E for the Cd solid solution, Cd–Zn eutectic solid solutions and the thermal conductivity of the eutectic liquid solution at T_E were measured for the Cd–Zn alloy.
(2) The equilibrated grain boundary, groove (cusp) shapes were obtained for the Cd solid solution Cd–Zn liquid solution using the radial heat flow apparatus and the Gibbs–Thomson coefficient was calculated by using the cusp shapes.
(3) The solid–liquid surface energy, σ_{SL}, was measured for the Cd solid solution Cd–Zn liquid solution by using the Gibbs–Thomson coefficient and the effective entropy change.
(4) The grain boundary energies, σ_{GB} were determined in Cd–Zn alloy.

Acknowledgments

This work was supported financially by Erciyes University Research Fund, project FBA-04-12. The authors would like to thank Erciyes University Technological Research and Development Centre for their technical support.

References

[1] Woodroff D P 1973 *The Solid–Liquid Interface* (Cambridge: Cambridge University Press) pp 1–4
[2] Gündüz M and Hunt J D 1985 *Acta Mater.* **33** 1651–72
[3] Gündüz M and Hunt J D 1989 *Acta Mater.* **37** 1839–45

[4] Maraşlı N 1994 *DPhil Thesis* Oxford University, England
[5] Maraşlı N and Hunt J D 1996 *Acta Mater.* **44** 1085–96
[6] Bayender B, Maraşlı N, Çadırlı E, Şişman H and Gündüz M 1998 *J. Cryst. Growth* **194** 119–24
[7] Bayender B, Maraşlı N, Çadırlı E and Gündüz M 1999 *Mater. Sci. Eng.* A **270** 343–8
[8] Maraşlı N, Keşlioğlu K and Arslan B 2003 *J. Cryst. Growth* **247** 613–22
[9] Keşlioğlu K and Maraşlı N 2004 *Mater. Sci. Eng.* A **369** 294–301
[10] Erol M, Maraşlı N, Keşlioğlu K and Gündüz M 2004 *Scr. Mater.* **51** 131–6
[11] Saatçi B 2000 *DPhil Thesis* Erciyes University, Turkey
[12] Touloukian Y S, Powell R W, Ho C Y and Klemens P G 1970 *Thermal Conductivity, Metallic Elements and Alloys* vol 1 (New York: Plenum) pp 45–9
[13] Keşlioğlu K, Erol M, Maraşlı N and Gündüz M 2004 *J. Alloys Compounds* **385** 207–13
[14] Hansen M and Anderko K 1985 *Constitutions of Binary Alloys* 2nd edn (New York: McGraw-Hill) pp 446–7
[15] Tassa M and Hunt J D 1976 *J. Cryst. Growth* **34** 38–48
[16] Waseda Y and Miller W A 1978 *Trans. JIM* **19** 546–52
[17] Jones H 2002 *Mater. Lett.* **53** 364–6